

6

MR perfusion imaging of the brain

S. Flacke
C. Manka
H. Urbach

Measurements of cerebral perfusion have become an important part of diagnostic imaging and therapy monitoring in a variety of brain diseases. Magnetic resonance perfusion imaging provides high-resolution images of various perfusion parameters in addition to the important morphological information acquired during the same imaging session. In conjunction with magnetic resonance imaging (MRI) diffusion-weighted imaging MR perfusion imaging has developed to a mainstay in early stroke imaging. The delineation of the so-called "tissue at risk" of ischemic damage characterized as a mismatch between alterations in diffusion-weighted and perfusion images is a key information if thrombolysis is a treatment option. Current ongoing clinical trials will show whether this information may allow to further extend the time window for thrombolytic therapy in stroke.

MR perfusion imaging allows the investigation of the well-established relationship between cerebral activity, metabolism, and regional hemodynamics. Under a wide range of physiological conditions the cerebral blood flow (CBF) is maintained at a constant level to provide a sufficient oxygen and glucose supply to the brain. This autoregulatory control is affected by the small cerebral arterioles, which are able to reduce the vascular resistance by widening of arterial sphincters and consecutive dilatation of small veins to maintain normal cerebral flow even under conditions where the systemic arterial blood pressure is as low as 70 mm Hg. A further drop of the perfusion pressure results in a CBF decrease, which is partly compensated with a higher oxygen extraction fraction and a reduction of cellular metabolism and energy demand. Irreversible tissue damage occurs if CBF drops below 10–12 mL/100 g of brain tissue per minute.

The complexity of these CBF patterns and autoregulatory control in various cerebrovascular diseases require the assessment of different parameters of cerebral perfusion, including the CBF, the cerebral blood volume, and the mean transit time (MTT). Considering these various parameters of cerebral perfusion, different stages of

impaired brain perfusion can be identified. The dilatation of small arteries, as the initial reaction to compensate for a reduced perfusion pressure, would increase the cerebral blood volume and to a certain extent the MTT while maintaining CBF at a constant level. This pattern is known as stage-one cerebral ischemia. With a decreasing perfusion pressure, the cerebral blood volume and the MTT will further increase; however, the CBF can no longer be kept at a constant level and will progressively decrease. This latter perfusion pattern is described as stage-two cerebral ischemia. If CBF falls beneath the critical level (stage three), irreversible damage to brain parenchyma will occur. Positron emission tomography (PET) and 133-xenon computed tomography (CT) can visualize and absolutely quantify these changes. However, both methods remain largely impractical for routine and emergency clinical use. Single photon emission tomography based on the detection of the distribution of 99m-technetium labeled hexamethylpropyleneamine oxime is a widely used method, although provided data are only relative indicators, and model-based calculation of CBF, cerebral blood volume, and MTT is imprecise. The potential of MRI to delineate the different perfusion parameters has been extensively evaluated in the recent years and the advantages of a multimodal MRI approach to various cerebrovascular disorders and cerebral tumors have been underlined.

In general, MRI offers two generic approaches to determine cerebral perfusion parameters. First, the blood flowing into an imaging slice can be marked either by magnetically tagging the selected slice or by the blood flowing into it. These techniques of arterial spin labeling are time-consuming, and measurable signal changes in states of reduced flow are usually small. However, if time is not a constraint, these techniques are promising especially if hemodynamic responses to various stimuli are studied during the same MRI study or breakdown of the blood-brain barrier compromises contrast-agent-based methods.

CHAPTER 6

The second approach uses fast dynamic acquisition to monitor signal changes during the passage of a bolus of contrast agent through the brain parenchyma. Presuming an intact blood–brain barrier and fast contrast injection signal changes during the first passage through the brain allow the quantification of the various perfusion parameters. In principle, T1- as well as T2*-dependent properties of the applied contrast agent can be used. T1-weighted images require small quantities of contrast but images are greatly affected by a breakdown of the blood–brain barrier and produce only relatively poor signal-to-noise ratios. Therefore, susceptibility-based brain perfusion imaging has become a widespread tool for the assessment of cerebral perfusion. During the passage through the brain the contrast agent cannot pass the intact blood–brain barrier and T2*-weighted sequences provide a good means of contrast because the compartmentalized susceptibility differences in the blood pool create microscopic field gradients that extend into the tissue and enhance T2*-dephasing, rendering the tissue dark. Relative regional cerebral blood volume (rCBV), time of bolus arrival, and bolus peak can be derived in a straightforward manner based on tracer kinetics theory, assuming that the change in relaxivity ($\Delta R2^* = 1/\Delta T2^*$) is proportional to the time-dependent contrast agent concentration: $\Delta R2^*(t) = k[\text{contrast agent}]$, where k is a field strength and pulse sequence specific constant. Presuming a monoexponential behavior, the signal intensity changes can be converted into concentration time curves ($C_{\text{meas}}(t) = -\ln(S(t)/S_0)/(kTE)$), where S_0 is the baseline signal before injection, and $S(t)$ the tissue signal present at time t . These concentration time curves need to be subsequently fitted to a gamma-variate function to correct for recirculation. From the fit parameters, the different perfusion parameters can be computed on a voxel-by-voxel basis and graphically represented in perfusion parameter maps. These include the relative rCBV map calculated by simple integration of the concentration versus time curve; the MTT map—a flow-dependent measure—which is calculated by dividing the integral of concentration–time curve by its height; the regional cerebral blood flow index as the ratio of volume and transit time; the time of bolus arrival (T0) map; and the time to bolus peak (TTP). Like single photon emission tomography, this technique does not provide absolute measures for CBV and CBF, which means that no comparison to normal values can be made. However, intraindividual perfusion changes can be readily and quickly visualized and the derived data closely correlate to data acquired by other imaging modalities (Figure 1).

Besides this straightforward calculation of relative perfusion data, MRI data can also be used for absolute quantification. However, absolute quantification requires the

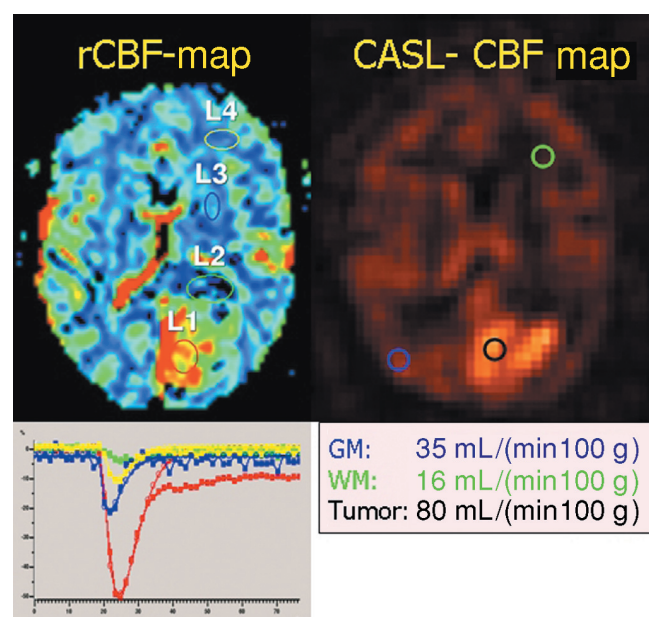


Figure 1 The figure shows a comparison of susceptibility-based perfusion imaging and continuous arterial spin labeling (CASL) perfusion imaging in a patient with a hyperperfused meningioma imaged at 3 T. Flow maps of both methods clearly identify the hyperperfused tumor. Concentration–time curves are displayed for various brain regions. With CASL absolute flow measures can be derived. (GM, grey matter; WM, white matter).

simultaneous registration of an arterial input function and modeling the vascular architecture, which is mathematically expressed through the residue function $R(t)$. The residue function describes how an impulse is retained in the vasculature as a function of time. The concentration of a tracer in a given volume of interest can then be expressed as a function of flow, arterial input, and the residue function. Although this approach has various inherent difficulties as there is no a priori knowledge of the diseased vessel architecture, numerical approaches (such as fast Fourier transform and singular value decomposition) to calculate the deconvolution of concentration–time curves with the arterial input function have shown similar results compared to quantified PET measurements. However, these very promising numerical approaches to derive quantitative MRI perfusion data still have limitations in the diseased vasculature. Deconvolution techniques are still sensitive to dispersion and, in some cases, to delays of the arterial input downstream of where it is measured. In such cases in which the blood reaches the tissue through collaterals, the chosen arterial input is not truly representative and may cause underestimation of the MTT. Unlike the determination of relative perfusion measurements, the calculation of quantitative data requires a more extensive computation that is not readily available at all clinical scanners for the emergency setting of stroke

imaging. Furthermore, an appropriate imaging technique has to be selected to correctly image the arterial input function.

The requirement for high temporal resolution has led to widespread use of echo planar imaging techniques (EPI). Single-shot and segmented EPI techniques are the most commonly used. T2*-sensitive 3D whole brain perfusion imaging has also become available. With the more widespread use of higher field MRI scanners, the imminent increase of susceptibility at higher magnetic field strength has led to a further improvement of these imaging techniques by either increasing the temporal resolution to subsecond imaging or reducing the amount of contrast agent required.

To date, the choice of the best imaging technique, i.e., T1-EPI, T2*-EPI, T2*-Presto, remains a fundamental question as it affects the sensitivity of the imaging experiment to blood vessel size, i.e., small capillaries or larger arteries.

Clinical application of MR perfusion imaging

Modern approaches to patients with acute ischemic stroke have emphasized early diagnosis and management since the recognition that early cerebral infarction may be in part reversible. Roughly 80% of ischemic infarcts are caused by thromboembolic occlusions of intracranial arteries of one of the major cerebral vessels; however, the extent of brain damage as a result of inadequate (stage three) perfusion is usually smaller than the affected vessel territory. Collateral circulation may provide sufficient energy and oxygen supply to parts of the affected vessel territory, which allows it to maintain basic functional cellular activity. With their high sensitivity to acute cerebral infarction, the combined use of echo planar diffusion-weighted and perfusion imaging has gained a major role. Diffusion imaging detects early diffusion changes associated with cytotoxic edema following energy metabolism failure and disruption of ion homeostasis. Perfusion has the potential to characterize the degree of regional hypoperfusion, which seems to be an important prognostic factor to determine final infarct extension (Figure 2).

In our series of patients with acute stroke, the areas of a significantly reduced rCBV in conjunction with a prolonged MTT were good predictors for final infarct size and clinical outcome in spontaneously developing stroke. However, if thrombolysis is a treatment option, MRI alone may refine selection of candidates. Identification of vessel obstruction and exclusion of hemorrhage,

the most important differential diagnosis of acute stroke, can be readily performed within minutes in the MR scanner. A perfusion–diffusion mismatch, which indicates tissue with decreased perfusion extending beyond that of diffusion abnormalities, is thought to represent tissue at risk of infarction, which is potentially salvageable with successful systemic or local thrombolysis. Such mismatches can be present even if vascular occlusion cannot be demonstrated. The effect of thrombolysis with regards to penumbral salvage has been found to be more pronounced if a mismatch is present. The degree of hypoperfusion in the mismatch area as defined by MRI perfusion parameter maps, first of all the MTT maps, seems to provide a more important information in clinical decision making than the time of treatment after stroke onset. Therefore the identification of thresholds for various perfusion parameters has been proposed, but it is still a matter of controversy. MTT prolongations of more than 22% compared to salvaged regions as well as TTP prolongation of more than 6 seconds were found in areas of later infarction and thus considered as critical levels. Nevertheless, absolute thresholds should still be considered cautiously as even a less severe hypoperfusion may lead to ischemic damage if the duration of hypoperfusion is long enough. Thus, reperfusion either spontaneous or post treatment has a great impact on tissue fate. Ongoing studies will show whether information derived from MRI perfusion and diffusion imaging may allow to further extend the time window for thrombolytic therapy in stroke. To date, thrombolytic treatment without the visualization of a perfusion deficit can only be used within the time constraints of early stroke studies.

MRI perfusion imaging has also been used with increasing interest to assess patients with extracranial vascular disease, especially patients with carotid vessel disease. Plaque formation within the vessel lumen is the origin of thromboemboli in a large group of patients. Although there is evidence that the severity of stenosis correlates with the incidence of thromboembolism, the degree of stenosis does not correlate to the amount of hypoperfusion downstream to the occlusion and to the risk of hypoperfusional infarcts. The risk of hypoperfusional infarcts is determined by the amount of collateral circulation available, which varies among patients according to the individual anatomy of the circle of Willis and further leptomeningeal collateralization. However, the risk of hypoperfusional infarcts can be assessed by imaging the regional cerebral perfusion. MRI has the ability to delineate these changes and to depict perfusion abnormalities. However, if relative values are provided, results may be misleading in the presence of bilateral carotid vessel disease. Intraindividual comparison of perfusion parameters

CHAPTER 6

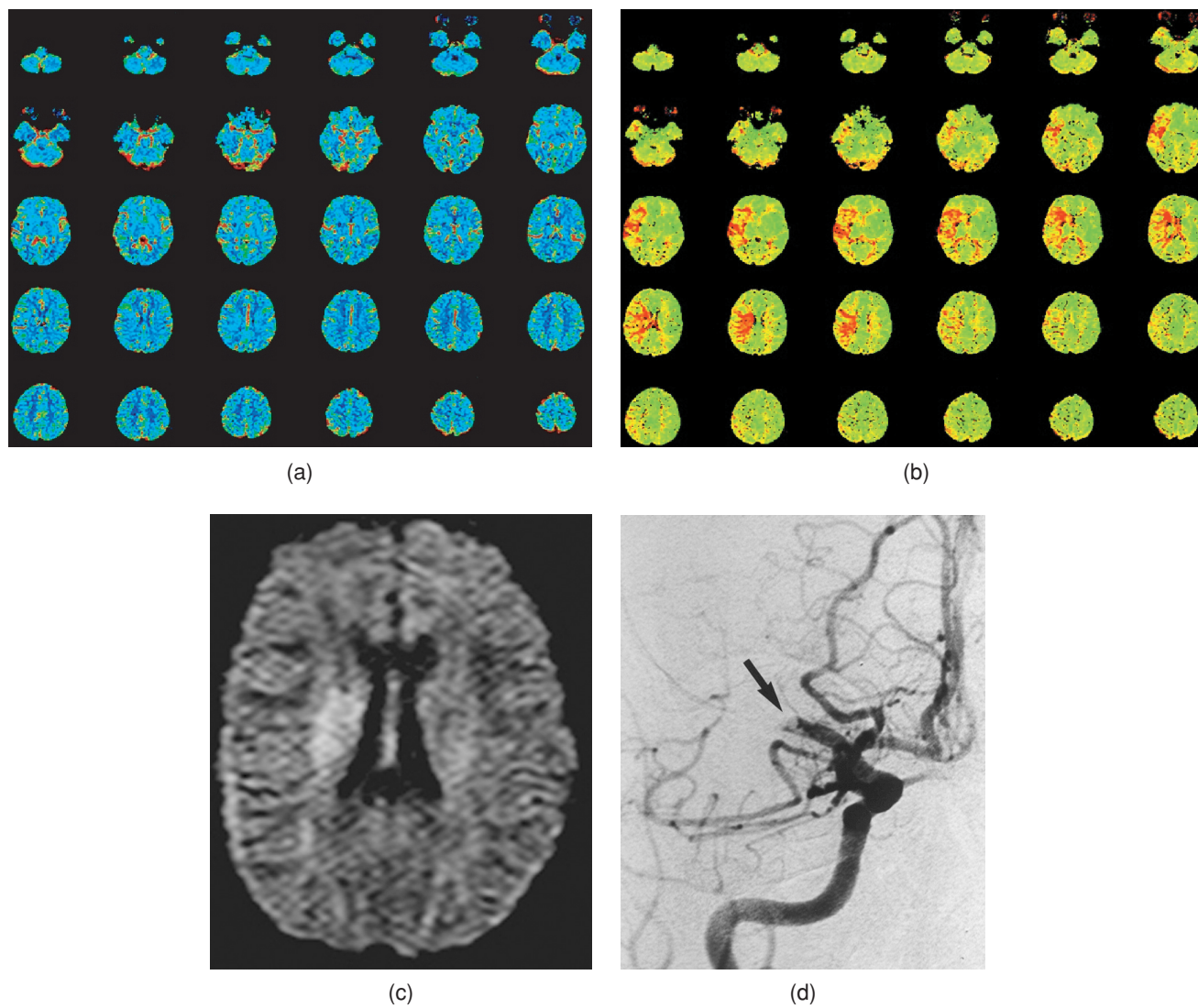


Figure 2 Parts (a) and (b) show the perfusion parameter maps of a patient with acute middle cerebral artery (MCA) occlusion imaged within the time window for intraarterial thrombolysis. On the rCBV map (a) there is only a small perfusion deficit within the right basal ganglia corresponding to an early diffusion-weighted imaging abnormality (c). The cortex of the right

MCA territory demonstrates no differences on rCBV maps compared to the contralateral side. However, TTP maps (b) show a large area of hypoperfusion in the right MCA territory. This mismatch area between diffusion-weighted imaging and perfusion imaging is large enough to justify thrombolysis. The corresponding angiogram (d) clearly shows the occlusion of the MCA (arrow).

before and after therapy or in combination with vascular dilatory challenge, such as acetazolamide, to characterize the individual cerebral perfusion reserve capacities is a reliable method.

MR perfusion imaging can further be applied in any brain disease where regional abnormalities of CBF are suspected (Figure 3). Small vessel diseases, arteriovenous malformations, the various types of dementia, and tumor vascularization are under ongoing investigation. It is likely that the shortcomings of relative MRI perfusion data will be overcome in the near future when postpro-

cessing programs will be implemented on routine clinical scanners, and absolute quantification of perfusion data may add information to the differential diagnosis of these various diseases. In addition, the use of blood pool agents that do not suffer from diffusion across the vascular endothelium and concomitant contrast changes, once they will be available for clinical first-pass imaging, will further increase the accuracy of MRI rCBV and CBF measurements.

MR perfusion imaging has yet evolved to a mainstay of neuroimaging.

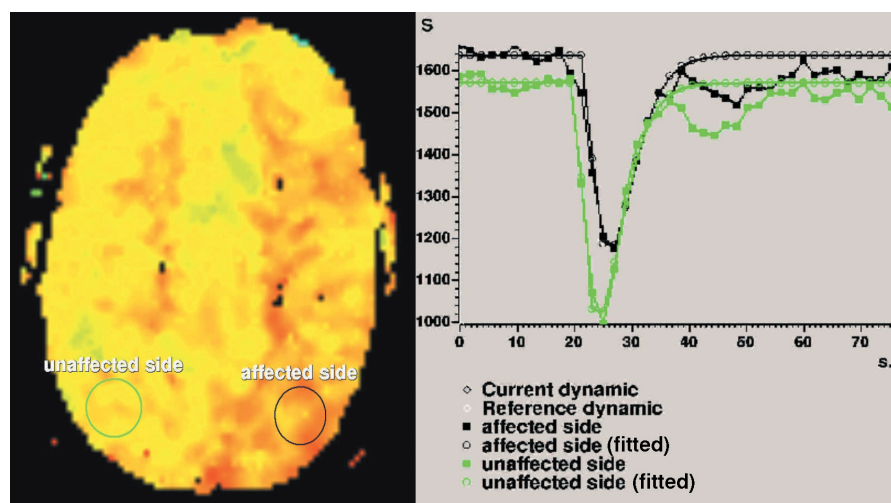


Figure 3 A Time-to-peak map of a patient with acute symptomatic migraine demonstrates a delayed bolus arrival in the posterior middle cerebral and the posterior cerebral artery territory. Regions of interest and the cor-

responding concentration–time curves are displayed. The hypoperfusion of the affected side can be clearly seen. The effect of gamma-variate fitting to correct for recirculation is shown.

Bibliography

Original publications

- Barber PA, Darby DG, Desmonds PM, et al. Prediction of stroke outcome with echo planar perfusion- and diffusion-weighted MRI. *Neurology* 1998; 51: 418–426.
- Bassingthwaite JB, Chan IS, Goldstein AA. An efficient method for smoothing indicator-dilution and other unimodal curves. *Comput Biomed Res* 1988; 21: 192–202.
- Boxerman JL, Rosen BR, Weisskoff RM. Signal-to-noise analysis of cerebral blood volume maps from dynamic NMR imaging studies. *J Magn Reson Imaging* 1997; 7: 528–537.
- Branch CA, Hernandez L, Yongbi M, Huang NC, Helpert JA. Rapid and continuous monitoring of cerebral perfusion by magnetic resonance line scan assessment with arterial spin tagging. *NMR Biomed* 1999; 12: 15–25.
- Butcher K, Parsons M, Baird T, et al. Perfusion thresholds in acute stroke thrombolysis. *Stroke* 2003; 34(9): 2159–2164.
- Campbell AM, Beaulieu C. Pulsed arterial spin labeling parameter optimization for an elderly population. *J Magn Reson Imaging* 2006; 23(3): 398–403.
- Chen JJ, Frayne R, Smith MR. Reassessing the clinical efficacy of two MR quantitative DSC PWI CBF algorithms following cross-calibration with PET images. *Phys Med Biol* 2005; 50(6): 1251–1263.
- Cutrer FM, Sorensen AG, Weisskoff RM, et al. Perfusion-weighted imaging defects during spontaneous migrainous aura. *Ann Neurol* 1998; 3: 25–31.
- de Bazelaire C, Siauve N, Fournier L, et al. Comprehensive model for simultaneous MRI determination of perfusion and permeability using a blood-pool agent in rats rhabdomyosarcoma. *Eur Radiol* 2005; 15(12): 2497–2505.
- Engelhorn T, Doerfler A, Forsting M, Heusch G, Schulz R. Does a relative perfusion measure predict cerebral infarct size? *AJNR Am J Neuroradiol* 2005; 26(9): 2218–2223.
- Ernst T, Chang L, Itti L, Speck O. Correlation of regional cerebral blood flow from perfusion MRI and SPECT in normal subjects. *Magn Reson Imaging* 1999; 17: 349–354.
- Fiebach JB, Schellinger PD, Gass A, et al. Stroke magnetic resonance imaging is accurate in hyperacute intracerebral hemorrhage: a multicenter study on the validity of stroke imaging. *Stroke* 2004; 35(2): 502–506.
- Fisel CR, Ackerman JL, Buxton RB, et al. MR contrast due to microscopically heterogeneous magnetic susceptibility: numerical simulations and applications to cerebral physiology. *Magn Reson Med* 1991; 17: 336–347.
- Fisher M, Garcia JH. Evolving stroke and the ischemic penumbra. *Neurology* 1996; 47: 884–888.
- Flacke S, Keller E, Hartmann A, et al. Improved diagnosis of early cerebral infarct by the combined use of diffusion and perfusion. *Rofo* 1998; 168(5): 493–501.
- Flacke S, Urbach H, Block W, et al. Perfusion and molecular diffusion-weighted MR imaging of the brain: in vivo assessment of tissue alteration in cerebral ischemia. *Amino Acids* 2002; 23(1–3): 309–316.
- Flacke S, Urbach H, Folkers PJ, et al. Ultra-fast three-dimensional MR perfusion imaging of the entire brain in acute stroke assessment. *J Magn Reson Imaging* 2000; 11(3): 250–259.
- Flacke S, Urbach H, Keller E, et al. Middle cerebral artery (MCA) susceptibility sign at susceptibility-based perfusion MR imaging: clinical importance and comparison with hyperdense MCA sign at CT. *Radiology* 2000; 215(2): 476–482.
- Floyd TF, Ratcliffe SJ, Wang J, Resch B, Detre JA. Precision of the CASL-perfusion MRI technique for the measurement of cerebral blood flow in whole brain and vascular territories. *J Magn Reson Imaging* 2003; 18(6): 649–655.

CHAPTER 6

- Gauvrit JY, Delmaire C, Henon H, et al. Diffusion/perfusion-weighted magnetic resonance imaging after carotid angioplasty and stenting. *J Neurol* 2004; 251(9): 1060–1067.
- Heiss WD. Flow thresholds for functional and morphological damage of the brain tissue. *Stroke* 1983; 14: 329–331.
- Heiss WD, Sobesky J, Hesselmann V. Identifying thresholds for penumbra and irreversible tissue damage. *Stroke* 2004; 35(11, suppl 1): 2671–2674.
- Hjort N, Butcher K, Davis SM, et al., for the CLA Thrombolysis Investigators. Magnetic resonance imaging criteria for thrombolysis in acute cerebral infarct. *Stroke* 2005; 36(2): 388–397.
- Ibaraki M, Shimosegawa E, Toyoshima H, et al. Effect of regional tracer delay on CBF in healthy subjects measured with dynamic susceptibility contrast-enhanced MRI: comparison with 15O-PET. *Magn Reson Med Sci* 2005; 4(1): 27–34.
- Johnson DW, Stringer WA, Marks MP, Yonas H, Good WF, Gur D. Stable xenon CT cerebral blood flow imaging: rationale for and role in clinical decision making. *AJNR Am J Neuroradiol* 1991; 12: 201–213.
- Jones CE, Wolf RL, Detre JA, et al. Structural MRI of carotid artery atherosclerotic lesion burden and characterization of hemispheric cerebral blood flow before and after carotid endarterectomy. *NMR Biomed* 2006; 19(2): 198–208.
- Keller E, Flacke S, Urbach H, Schild HH. Diffusion- and perfusion-weighted magnetic resonance imaging in deep cerebral venous thrombosis. *Stroke* 1999; 30: 1144–1146.
- Kidwell CS, Hsia AW. Imaging of the brain and cerebral vasculature in patients with suspected stroke: advantages and disadvantages of CT and MRI. *Curr Neurol Neurosci Rep* 2006; 6(1): 9–16.
- Kimura H, Takeuchi H, Koshimoto Y, et al. Perfusion imaging of meningioma by using continuous arterial spin-labeling: comparison with dynamic susceptibility-weighted contrast-enhanced MR images and histopathologic features. *AJNR Am J Neuroradiol* January 2006; 27(1): 85–93.
- Liu G, Sobering G, Duyn J, Moonen C. A functional MRI technique combining principles of echo-shifting with a train of observations (PRESTO). *Magn Reson Med* 1993; 30: 764–768.
- Manka C, Traber F, Gieseke J, Schild HH, Kuhl CK. Three-dimensional dynamic susceptibility-weighted perfusion MR imaging at 3.0 T: feasibility and contrast agent dose. *Radiology* 2005; 234(3): 869–877.
- The National Institute of Neurological Disorders and Stroke rt-PA Stroke Study Group. Tissue plasminogen activator for acute ischemic stroke. *N Eng J Med* 1995; 333: 1581–1587.
- Neumann-Haefelin T, Wittsack HJ, Wenserski F, et al. Diffusion- and perfusion-weighted MRI. The DWI/PWI mismatch region in acute stroke. *Stroke* 1999; 30(8): 1591–1597.
- Ostergaard L. Principles of cerebral perfusion imaging by bolus tracking. *J Magn Reson Imaging* 2005; 22(6): 710–717.
- Ostergaard L, Smith DF, Vestergaard-Poulsen P, et al. Absolute cerebral blood flow and blood volume measurements by magnetic resonance imaging bolus tracking: comparison with PET values. *J Cereb Blood Flow Metab* 1998; 18: 425–432.
- Ostergaard L, Weiskoff RM, Chesler DA, Gyldensted C, Rosen BR. High resolution measurement of cerebral blood flow using intravascular tracer bolus passage. Part I: Mathematical approach and statistical analysis. *Magn Reson Med* 1996; 36: 715–725.
- Parsons MW, Barber PA, Chalk J, et al. Diffusion- and perfusion-weighted MRI response to thrombolysis in stroke. *Ann Neurol* 2002; 51(1): 28–37.
- Rashid W, Parkes LM, Ingle GT, et al. Abnormalities of cerebral perfusion in multiple sclerosis. *J Neurol Neurosurg Psychiatry* 2004; 75(9): 1288–1293.
- Rivers CS, Wardlaw JM, Armitage PA, et al. Do acute diffusion- and perfusion-weighted MRI lesions identify final infarct volume in ischemic stroke? *Stroke* 2006; 37(1): 98–104.
- Roberts DA, Detre JA, Bolinger L, Insko EK, Leigh JS, Jr. Quantitative magnetic resonance imaging of human brain perfusion at 1.5 T using steady-state inversion of arterial water. *Proc Natl Acad Sci USA* 1994; 91(1): 33–37.
- Rollin N, Guyotat J, Streichenberger N, Honnorat J, Tran Minh VA, Cotton F. Clinical relevance of diffusion and perfusion magnetic resonance imaging in assessing intra-axial brain tumors. *Neuroradiology* 2006; 10: 1–10.
- Röther J, Schellinger PD, Gass A, et al., for the Kompetenznetzwerk Schlaganfall Study Group. Effect of intravenous thrombolysis on MRI parameters and functional outcome in acute stroke <6 hours. *Stroke* 2002; 33(10): 2438–2445.
- Schellinger PD, Fiebach JB, Jansen O, et al. Stroke magnetic resonance imaging within 6 hours after onset of hyperacute cerebral ischemia. *Ann Neurol* 2001; 49(4): 460–469.
- Schellinger PD, Latour LL, Wu CS, Chalela JA, Warach S. The association between neurological deficit in acute ischemic stroke and mean transit time. Comparison of four different perfusion MRI algorithms. *Neuroradiology* 2006; 48(2): 69–77.
- Shih LC, Saver JL, Alger JR, et al. Perfusion-weighted magnetic resonance imaging thresholds identifying core, irreversibly infarcted tissue. *Stroke* 2003; 34(6): 1425–1430.
- Sims J, Schwamm LH. The evolving role of acute stroke imaging in intravenous thrombolytic therapy: patient selection and outcome assessment. *Neuroimaging Clin North Am* 2005; 15: 412–440.
- Sobesky J, Zaro Weber O, Lehnhardt FG, et al. Which time-to-peak threshold best identifies penumbral flow? A comparison of perfusion-weighted magnetic resonance imaging and positron emission tomography in acute ischemic stroke. *Stroke* 2004; 35(12): 2843–2847.
- Sobesky J, Zaro Weber O, Lehnhardt FG, et al. Does the mismatch match the penumbra? Magnetic resonance imaging and positron emission tomography in early ischemic stroke. *Stroke* 2005; 36(5): 980–985.
- Tanabe JL, Yongbi M, Branch C, Hrabe J, Johnson G, Helpert JA. MR perfusion imaging in human brain using the UNFAIR technique. Un-inverted flow-sensitive alternating inversion recovery. *J Magn Reson Imaging* 1999; 9: 761–767.
- Thilmann O, Larsson EM, Bjorkman-Burtscher IM, Stahlberg F, Wirestam R. Comparison of contrast agents with high molarity and with weak protein binding in cerebral perfusion imaging at 3 T. *J Magn Reson Imaging* 2005; 22(5): 597–604.
- Thomalla G, Schwark C, Sobesky J, et al. Outcome and symptomatic bleeding complications of intravenous thrombolysis within 6 hours in MRI-selected stroke patients. Comparison of a German Multicenter Study with the Pooled Data of ATLANTIS,

MR perfusion imaging of the brain

- ECASS and NINDS tPA Trials. *Stroke* March 2006; 37(3): 852–858.
- Thompson HK, Starmer CF, Whalen RE, McIntosh HD. Indicator transit time considered as a gamma variate. *Circ Res* 1964; 14: 502–515.
- Togao O, Mihara F, Yoshiura T, et al. Cerebral hemodynamics in Moyamoya disease: correlation between perfusion-weighted MR imaging and cerebral angiography. *AJNR Am J Neuroradiol* 2006; 27(2): 391–397.
- Villringer A, Rosen BR, Belliveau JW, et al. Dynamic imaging with lanthanide chelates in normal brain: contrast due to magnetic susceptibility effects. *Magn Reson Med* 1988; 6: 164–174.
- Wang J, Rao H, Wetmore GS, et al. Perfusion functional MRI reveals cerebral blood flow pattern under psychological stress. *Proc Natl Acad Sci USA* 2005; 102(49): 17804–17809.
- Weisskoff RM, Chesler D, Boxerman JL, Rosen BR. Pitfalls in MR measurements of tissue blood flow with intravascular tracers: Which mean transit time? *Magn Reson Med* 1993; 23: 553–559.
- Wong EC, Buxton RB, Frank LR. Quantitative perfusion imaging using arterial spin labeling. *Neuroimaging Clin North Am* 1999; 9: 333–342.
- Zhu XP, Li KL, Kamaly-Asl ID, et al. Quantification of endothelial permeability, leakage space and blood volume in brain tumors using combined T1 and T2* contrast enhanced dynamic MR imaging. *J Magn Reson Imaging* 2000; 11: 575–585.
- Zierler KL. Theoretical basis of indicator-dilution methods for measuring blood flow and volume. *Circ Res* 1965; 16: 393–407.

